

Article

Effects of the Combination of Chemical Pretreatments and Dry Grinding of the *Arundo donax* L. Plant

Patricia O. Schmitt ¹, Débora da S. Rodrigues ², Matheus de P. Goularte ², Silvia H. F. da Silva ¹,
Marcilio M. Morais ³, Darci A. Gatto ¹, Cláudia F. Lemons e Silva ², Camila M. Cholant ¹
and André L. Missio ^{1,*}

¹ Postgraduate Program in Materials Science and Engineering, Federal University of Pelotas, Pelotas 96010-610, RS, Brazil; patricia.olimitt@gmail.com (P.O.S.); silviahfuentes@hotmail.com (S.H.F.d.S.); darcigatto@yahoo.com (D.A.G.); camila.scholant@gmail.com (C.M.C.)

² Engineering Center, Federal University of Pelotas, Pelotas 96010-450, RS, Brazil; deborar999@gmail.com (D.d.S.R.); almatheusgoularte@gmail.com (M.d.P.G.); lemonsclau@gmail.com (C.F.L.e.S.)

³ Chemical Engineering, Federal University of Pampa, Bagé 96413-172, RS, Brazil; marciliomorais@unipampa.edu.br

* Correspondence: andre.missio@ufpel.edu.br

Abstract: *Arundo donax* L. is a plant with great potential as lignocellulosic biomass, being a promising source for the development of biodegradable materials. This study evaluated the effects of different chemical pretreatments (H₂SO₄, NaOH, and NaClO) combined with dry milling on the physicochemical properties of biomass. Pretreatment with NaClO was the most effective in removing lignin, reducing its content to 0.2%, while increasing the cellulose content to 67%. Pretreatment with H₂SO₄, although retaining a higher lignin content (24%), resulted in the greatest reduction in particle size, reaching a mean diameter (D_m) of 44.31 μm after 20 h of milling. Density analysis revealed that the raw samples reached a maximum density of 0.218 g/cm³ after 20 h of milling, with the pretreated samples showing lower densities due to the removal of structural components. Thermal analysis showed mass losses of up to 66.4% for samples pretreated with NaClO after 10 h of milling, indicating significant structural changes and improved thermal stability. Morphological analysis via SEM demonstrated elongated and fine particles, with acid pretreatment resulting in the most pronounced structural changes. These findings highlight the efficiency of combining chemical and physical pretreatments to modify the structure of *A. donax* L., optimizing its properties for the production of high-performance biodegradable materials.

Keywords: biomass; lignocellulosic; *Arundo donax* L.; chemical delignification; ball mill; particle size distribution



Academic Editor: Valentina Sessini

Received: 15 October 2024

Revised: 11 December 2024

Accepted: 15 January 2025

Published: 19 January 2025

Citation: Schmitt, P.O.; Rodrigues, D.d.S.; Goularte, M.d.P.; da Silva, S.H.F.; Morais, M.M.; Gatto, D.A.; Silva, C.F.L.e.; Cholant, C.M.; Missio, A.L. Effects of the Combination of Chemical Pretreatments and Dry Grinding of the *Arundo donax* L. Plant. *Macromol* **2025**, *5*, 4. <https://doi.org/10.3390/macromol5010004>

Copyright: © 2025 by the authors. Licensee MDPI, Basel, Switzerland. This article is an open access article distributed under the terms and conditions of the Creative Commons Attribution (CC BY) license (<https://creativecommons.org/licenses/by/4.0/>).

1. Introduction

The plant *Arundo donax* L., known for its extreme adaptability and proliferation in tropical, subtropical, and temperate climates, is an invasive species that occupies vast areas, causing significant environmental impacts in several regions around the world [1,2]. However, its abundance and rapid biomass accumulation make it a promising source of renewable raw materials, especially in the field of lignocellulosic materials [3]. Its biomass is mainly composed of cellulose, hemicellulose, lignin, and biopolymers that can be transformed into high value-added products for various applications [4,5].

The growing demand for sustainable materials, especially from agricultural and forestry residues and invasive plant species, has encouraged the search for alternative raw

materials that promote environmental sustainability and reduce dependence on petroleum-derived materials. In this scenario, the comparison between different lignocellulosic biomasses reveals valuable information about the potential of *Arundo donax* L. as a renewable source of materials.

Switchgrass, known for its high biomass yield and adaptability, stands out in the production of bioenergy and biofuels due to its lignocellulosic composition, which favors fermentation processes—the same characteristic observed in *Arundo donax* L. [3]. Bamboo, widely valued for its rapid growth and high tensile strength, has consolidated applications in sustainable construction materials, with fibers that present properties similar to those of *Arundo donax* L., which also demonstrate high potential in the production of high-quality cellulose [6].

These comparisons reinforce the position of *Arundo donax* L. as a prominent biomass, capable of meeting the growing demand for renewable materials in sectors such as sustainable construction, bioenergy, and biorefineries, offering competitive and environmentally responsible solutions. Furthermore, the lignocellulosic biomass of *Arundo donax* L. has stood out for its wide availability and benefits, gaining both scientific and industrial relevance [7–9]. This natural resource is used in several applications, including paper manufacturing [4], civil construction [5], phytoremediation of soils contaminated by heavy metals [10], production of bioenergy and biofuels [7,11,12], and also in the development of sustainable packaging [13].

The appreciation of *Arundo donax* L. reinforces the importance of exploring its structural components and transforming them into products with greater added value. However, to add value, it is essential to deconstruct this lignocellulosic biomass and, sometimes, also reduce the size of the particles through pre-treatments (mechanical, chemical, physical–chemical, and biological) [14,15].

The transformation of lignocellulosic biomass requires the application of effective pretreatments to defibrillate its complex structure and release the desired components, such as cellulose and hemicellulose. Among the main pretreatment methods are chemical processes, which include the use of acids, bases, and oxidizing agents, each with a different purpose. Acid pretreatment, for example, is widely used to hydrolyze hemicellulose and partially decompose cellulose, facilitating the extraction of these fractions [16–19]. The alkaline pretreatment, using sodium hydroxide (NaOH), is a highly recalcitrant biopolymer, resulting in a solid fraction rich in cellulose and hemicellulose, presenting changes in the surface area, porosity and degree of crystallinity [14,20,21]. Finally, bleaching, usually performed with sodium hypochlorite (NaClO), is used to improve the purity and color of the cellulose by removing residual lignin [22,23].

In addition to chemical pretreatments, reducing the particle size of biomass by grinding is a critical step to improve the efficiency of conversion processes. Ball milling, in particular, has emerged as an effective technique for obtaining ultrafine particles with high surface area and improved reactivity [24]. This mechanical method offers significant advantages compared to other techniques, allowing controlled grinding that alters the physical and chemical properties of the biomass [25]. When applied to lignocellulosic materials, ball milling not only increases the surface area of the biomass, but also facilitates the interaction between the components and promotes a more homogeneous distribution of the cellulose, hemicellulose, and lignin fractions, which is crucial for the production of films with ideal characteristics [26].

Ball milling also plays an important role in the preparation of biodegradable films, especially when combined with chemical pretreatments. By reducing particle size and improving particle dispersion, this process results in more homogeneous and cohesive films with attractive mechanical and thermal properties [27]. This is particularly relevant

for the manufacture of biodegradable packaging, where the uniformity and strength of the films are essential factors in ensuring the quality and durability of the products [27].

Although *Arundo donax* L. biomass has been extensively investigated in previous studies for applications in biofuels [28], biocomposites [29], and sustainable materials [3], the literature presents a significant gap regarding the integrated assessment of the effects of chemical pretreatments and dry milling on its chemical, thermal, morphological, and structural properties. Existing studies tend to address the impact of a single chemical pretreatment or physical processing step in isolation, without exploring how these approaches can interact synergistically to efficiently modify the lignocellulosic structure.

This paper is a pioneer in investigating, in an integrated manner, the effects of different chemical pretreatments (acid, alkaline, and bleaching) combined with varying milling times on the structure and properties of *Arundo donax* L. biomass. The mechanistic approach employed allows for a detailed characterization of the changes in the lignocellulosic structure, with the aim of optimizing essential properties for the future development of high-performance biodegradable materials. In addition, this study contributes significantly to the valorization of agro-industrial waste by implementing sustainable practices aligned with the principles of a circular economy.

The valorization of *Arundo donax* L. as lignocellulosic biomass is directly related to the reduction in the ecological footprint of the materials sector, as it encourages the use of renewable resources and minimizes waste. In this context, the study demonstrates that the choice of optimized chemical pretreatment strategies and sustainable waste management is crucial to balance technical efficiency and environmental impacts. For urban development and the reduction in the ecological footprint, it is crucial to implement the Sustainable Development Goals, SDG SDG 12 (Responsible Consumption and Production), by providing more sustainable solutions for the use of biomass and chemicals; SDG 13 (Climate Action), by mitigating carbon emissions through the substitution of non-renewable materials; and SDG 15 (Life on Land), by promoting the control of invasive species and the conservation of ecosystems [30].

2. Materials and Methods

2.1. Materials

The *Arundo donax* L. (*A. donax* L.) plants were supplied by Embrapa Clima Temperado at the Cascata Experimental Station, located in the rural area of the municipality of Pelotas in Rio Grande do Sul (latitude 31°42' S, longitude 52°24' W). The reagents used in this study were sulfuric acid (H₂SO₄, technical grade 98%, Labsynth-Diadema/SP, Brazil), sodium hydroxide (NaOH, technical grade 98%, Dinâmica-Tatuapé/SP, Brazil), and sodium hypochlorite (NaClO, technical grade 6%, Dinâmica).

2.2. Chemical Pretreatment

The entire plant (stem, leaf) underwent prior conditioning in a greenhouse with air circulation at 60 °C for 7 days and was then ground in a knife mill (Marconi, MA 340). Subsequently, it was subjected to different chemical pretreatments (H₂SO₄, NaOH, and NaClO) to separate the majority of the constituents, such as cellulose, hemicellulose, lignin, and others. For acid pretreatment, 40 g of sample was combined with a 2% H₂SO₄ solution in a 1:10 (*w/v*) ratio in a glass vial with a lid and then autoclaved at 121 °C and 1 atm for 60 min. It was then vacuum-filtered and washed with hot water until a neutral pH was reached, followed by drying in an oven at 50 °C for 24 h [31]. The alkaline pretreatment with 7% NaOH was carried out under identical conditions, but lasting 30 min [32]. The bleaching pretreatment occurred in two stages. The first stage involved delignification as described in the alkaline pretreatment, but using 120 g of sample. The second stage was

based on the methodology described by [33]. For this purpose, a 2% NaClO solution was added to the sample, in a proportion of 1:10 (*w/v*), for 20 h at room temperature. It was then vacuum-filtered and washed with hot water until it reached a neutral pH before being placed in an oven at 50 °C for 24 h.

2.3. Physical Treatment in Ball Mill

After chemical pretreatment, the samples were sieved to obtain standardized particles with a 45 mesh sieve size (0.354 mm), which were called the control group [34]. In total, 20 g of sample from each chemical pretreatment was subjected to dry grinding in a ball mill (Quimis brand), with a capacity of 1 L, with porcelain balls of varying sizes, maintaining a material-to-ball ratio of 1:10, as illustrated in Figure 1. Grinding occurred at a rotation speed of 150 rpm for various grinding times (5, 10, and 20 h), followed again by sieving.

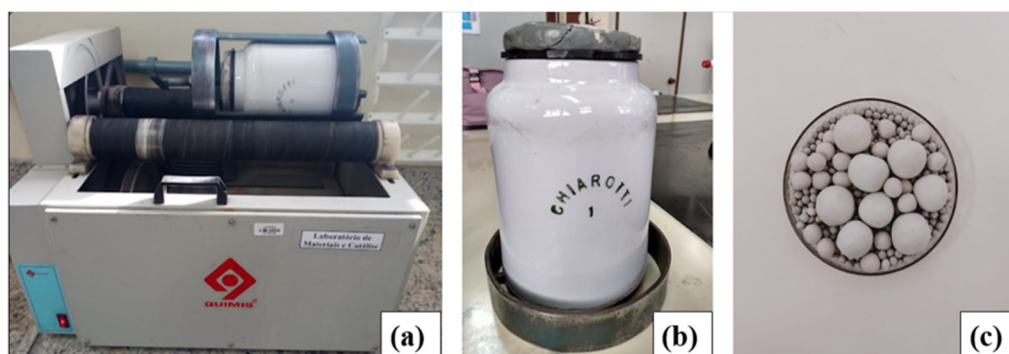


Figure 1. Photograph of the (a) ball mill, (b) porcelain jar, and (c) porcelain spheres of different sizes.

2.4. Characterization Techniques

2.4.1. Chemical Analysis

The chemical analysis was carried out in accordance with Technical Association of the Pulp and Paper Industry (TAPPI standards) [35], using the samples in powder form, after chemical pre-treatments. The following determinations were performed: ethanol-toluene extractive content, Klason lignin content, cellulose content, and holocellulose (remaining mass up to 100%), for quantification of inorganic materials. The results, present-ed as mean \pm SD, were analyzed with analysis of variance ANOVA and teste de significância de Fisher (least significant difference—LSD) to identify significant differences, using a significance level of 5% to compare the means between treatments and the control.

2.4.2. Colorimetric Analysis

To determine the colorimetric parameters, the CIELab system (L^* , a^* , b^*) was used, which consists of the following coordinates: luminosity (L^*), green-red axis (a^*), blue-yellow axis (b^*) [36,37]. A CR-400 colorimeter (Konica Minolta, Tokyo, Japan) was used, with an observation angle of 10°, calibrated with the porcelain calibrator and configured with D65 light, to determine the color of the powders.

The following colorimetric parameters were analyzed: luminosity (L^*) (the closer to 100, the lighter the color and the closer to 0, the darker), green-red coordinate (a^*) (negative markings indicate green colors, positive markings indicate red colors), and blue-yellow coordinate (b^*) (negative markings indicate blue colors, positive markings indicate yellow colors). For the analysis of color changes (ΔE), Equation (1) [36] was used:

$$\Delta E = \sqrt{(\Delta L^2 + \Delta a^2 + \Delta b^2)} \quad (1)$$

where ΔE is the variation of all colors, ΔL is the variation of lightness, Δa is the variation of the red-green coordinate, and Δb is the variation of the blue-yellow coordinate.

2.4.3. Density Analysis

Density is determined by the relationship between the mass (m) and volume (V) of the material. Mass is measured in grams (g) and volume in cubic centimeters (cm^3), according to Equation (2) [38]. For particulate materials, volume is calculated using a cylindrical container, considering the radius (r) of the container and the height (h) of the sample.

$$\rho = \frac{m}{V} \text{ e } V = r^2 * h \quad (2)$$

2.4.4. Granulometric Distribution Analysis

The particle size distribution analysis was conducted using a laser diffraction analyzer (CILAS 1064 model, Vila Cruzeiro/SP, Brazil), designed to measure particles within the range of 0.04 to 500 μm . The methodology followed the manufacturer's guidelines to ensure precision and reliability. Samples were dispersed in deionized water and subjected to 60 s of ultrasound prior to measurements, which effectively minimized particle agglomeration. The results were reported in terms of mean particle diameter (D_m) and cumulative distribution values (D_{10} , D_{50} , and D_{90}), providing a comprehensive characterization of the particle size distribution. Each sample underwent five independent measurements to enhance accuracy and reproducibility. The selection of five measurements aligns with established analytical best practices and meets the specific requirements for the granulometric characterization of lignocellulosic materials. This approach ensures robust and representative data for subsequent analyses.

2.4.5. Morphological Analysis

The morphological analysis of the samples was performed using a scanning electron microscope (SEM, model JOEL JSM-6610LV), operating at a beam current of 1 pA and a voltage of 15 kV. Images were obtained at magnification up to $\times 100$, allowing detailed observation of the particle surface and providing information on the morphology and structure of the samples at the microscopic level. Sample preparation included gold metallization to improve electrical conductivity and allow high-resolution analyses, based on the study carried out by Ribeiro et al. (2023) [39].

2.4.6. Thermal Analysis

The thermal stability of the samples was analyzed by thermogravimetric (TG) analysis using a Shimadzu DTG-60 thermogravimetric analyzer. The method followed the ASTM E1131-08 standard [40] for determining the thermal properties of solid materials. The samples were heated from 25 to 800 $^{\circ}\text{C}$ at a heating rate of 10 $^{\circ}\text{C}/\text{min}$, under an inert nitrogen (N_2) atmosphere, with a flow rate of 50 mL/min. This approach was adopted to ensure controlled and reproducible experimental conditions, allowing the accurate characterization of the thermal decomposition and stability of the biomass components.

2.4.7. FTIR Analysis

The chemical properties of the samples were evaluated by Fourier transform infrared spectroscopy (FTIR) coupled to an attenuated total reflection (ATR) device, using a Shimadzu Prestige-21 spectrometer. The analysis was performed in the range of 400–4000 cm^{-1} , with a spectral resolution of 4 cm^{-1} , according to the guidelines established by the ASTM E1252-13 standard [41] for infrared spectroscopy. This methodology allows the identification of the main functional groups present in the samples and the

evaluation of the structural modifications caused by the different treatments applied to the biomass.

2.4.8. XRD Analysis

X-ray diffraction (XRD) allowed the crystallinity of the different samples to be characterized, using a Bruker D8 Advance diffractometer with CuK α radiation ($\lambda = 1.54 \text{ \AA}$) with Bragg–Brentano geometry and operated at 40 kV and 20 mA. The crystallinity index (IC%) was determined based on the reflected intensity data following the method of Segal et al., 1959 [42], according to Equation (3):

$$IC\% = \frac{I_{200} - I_{am}}{I_{200}} \times 100 \quad (3)$$

where I_{002} corresponds to the crystalline portion of the sample located at a diffraction angle around $2\theta = 22^\circ$, and I_{am} is the peak intensity of the amorphous part measured as the lowest intensity at a diffraction angle around $2\theta = 15^\circ$.

3. Results and Discussion

3.1. Chemical Analysis

Figure 2 shows the chemical characterization of *A. donax* L. samples after different chemical pretreatments: *in natura*, H₂SO₄, NaOH, and NaClO, highlight the extractive fractions, lignin, hemicellulose, and cellulose. Chemical characterization analyses of the samples *in natura* and after chemical pretreatments revealed significant changes in the composition of non-cellulosic materials.

The extractive contents obtained were 6% for the *in natura* sample, 5% for that treated with H₂SO₄, 7% for NaOH, and 1% for NaClO. Pretreatment with NaClO proved to be highly efficient in removing compounds from the extractive fraction when compared to the *in natura* biomass. This effect is due to the removal of lipids, non-structural sugars, and the process of volatilization and degradation of extractives [42,43].

Regarding lignin, the sample treated with H₂SO₄ presented a content of 24%, higher than the other pre-treatments: *in natura* (14%), NaOH (12%), and NaClO (0.2%). The high lignin content in the acid pretreatment is attributed to the depolymerization of the cellulosic and hemicellulosic structures, in addition to the removal of extractive compounds, although it has shown low efficiency in lignin hydrolysis [44,45]. On the other hand, pretreatment with NaClO completely degraded lignin, showing efficiency in bleaching, with less impact on hemicellulose and cellulose [46].

The hemicellulose content was 29% for the *in natura* sample, while the values for H₂SO₄, NaOH, and NaClO were 24%, 21%, and 17%, respectively. This reduction is attributed to the hydrolysis of hemicelluloses into sugars and degradation products, a characteristic of pretreatments [45]. Studies report that the reduction in hemicellulose improves the efficiency of enzymatic conversion processes, being relevant for biofuel and biochemical industries [47].

All pretreatments presented high cellulose contents due to the resistance of the crystalline structure of cellulose to degradation [48]. The highest content was observed in the pretreatment with NaClO (67%), followed by NaOH (39%), *in natura* (32%), and H₂SO₄ (28%). The bleaching process aims to remove unwanted components, such as lignin and hemicellulose, making the cellulose more accessible for further processing [49]. These treatments are promising for the production of cellulose-rich films, with potential for application in biodegradable materials [50].

These results highlight the fundamental role of pretreatments in modifying the macromolecules of lignocellulosic biomass, directly influencing the mechanical and structural properties of the material.

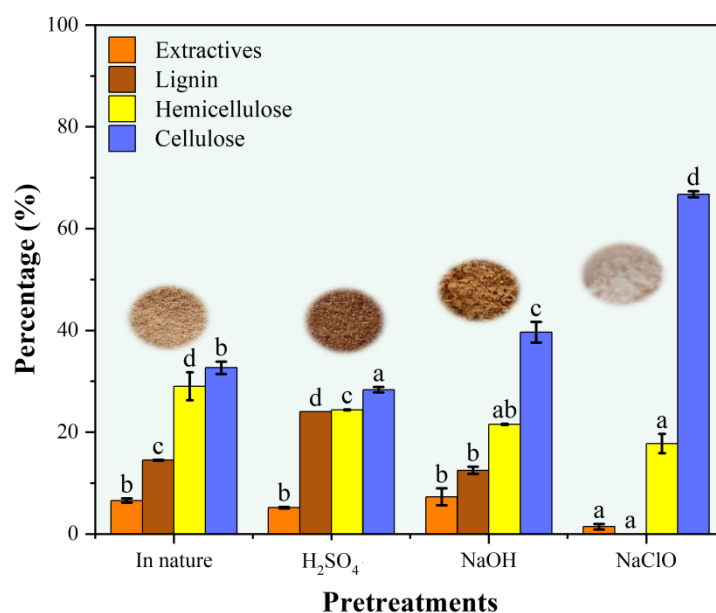


Figure 2. Chemical characterization of the samples (different letters above the bars indicate a statistically significant difference). Note: The vertical lines represent the standard deviation of each pretreatment.

3.2. Colorimetric Analysis

Figure 3 illustrates photographic images of samples subjected to different chemical pretreatments before and after grinding for 20 h. Overall, there is a noticeable change to the naked eye in tones and colors. Arundo in natura (Figure 3a,e) and those pretreated with NaOH (Figure 3c,g) exhibited brown coloration, although of a lighter tone compared to those subjected to pretreatment with H₂SO₄ (Figure 3b,f). This is attributed to the chromophoric groups present in lignin [51]. In this regard, as expected, the samples pretreated with NaClO (Figure 3d,h) presented a white coloration, indicative of lignin removal.

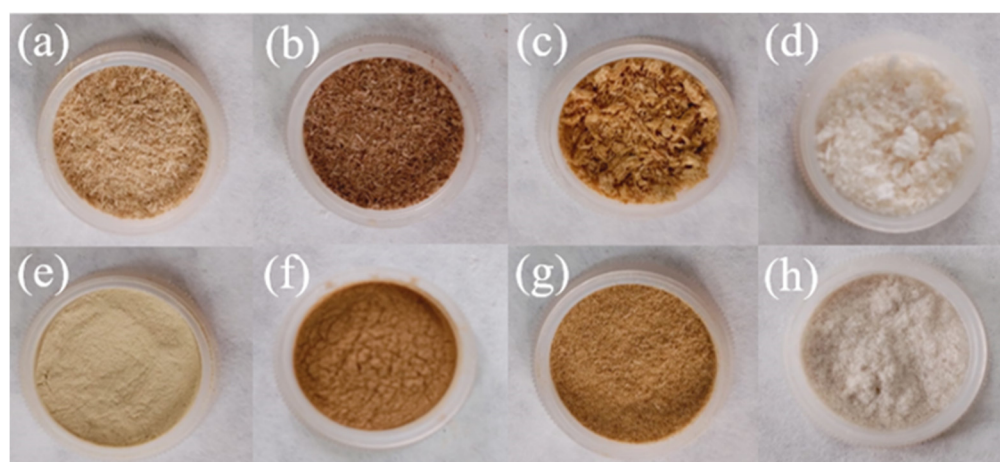


Figure 3. Photograph of *A. donax* L. (a–e) in natura and, pretreated: (b–f) H₂SO₄, (c–g) NaOH e (d–h) NaClO, 0 h (control), and 20 h of bottom grinding paper.

Colorimetric analysis (Figure 4) was performed using the CIELab method to accurately determine the effect of colors. When comparing the luminosity results in Figure 4a (0 = black and 100 = white), it is observed that the samples pre-treated with H_2SO_4 presented the lowest luminosity, as this chemical pre-treatment is used to remove the holo-cellulose present in the biomass, mainly those with lower molecular weight, leaving only lignin [32,52]. The samples pretreated with NaOH also presented low luminosity due to only partial removal of lignin. In contrast, those pretreated with NaClO presented higher luminosity. These results corroborate the images observed in Figure 3. Figure 4b,c show the variations in chromaticity of the samples subjected to 20 h of milling in relation to their respective controls. These variations after long milling times can be attributed to changes in the chromophore groups belonging to lignin and extractives [53,54] due to friction during milling. However, due to the human eye's difficulty in distinguishing certain colors, the calculation of the color variation is shown in Figure 4d, and allows determination that there was color variation both between the pretreatments and between the sample subjected to 20 h of milling and its respective control.

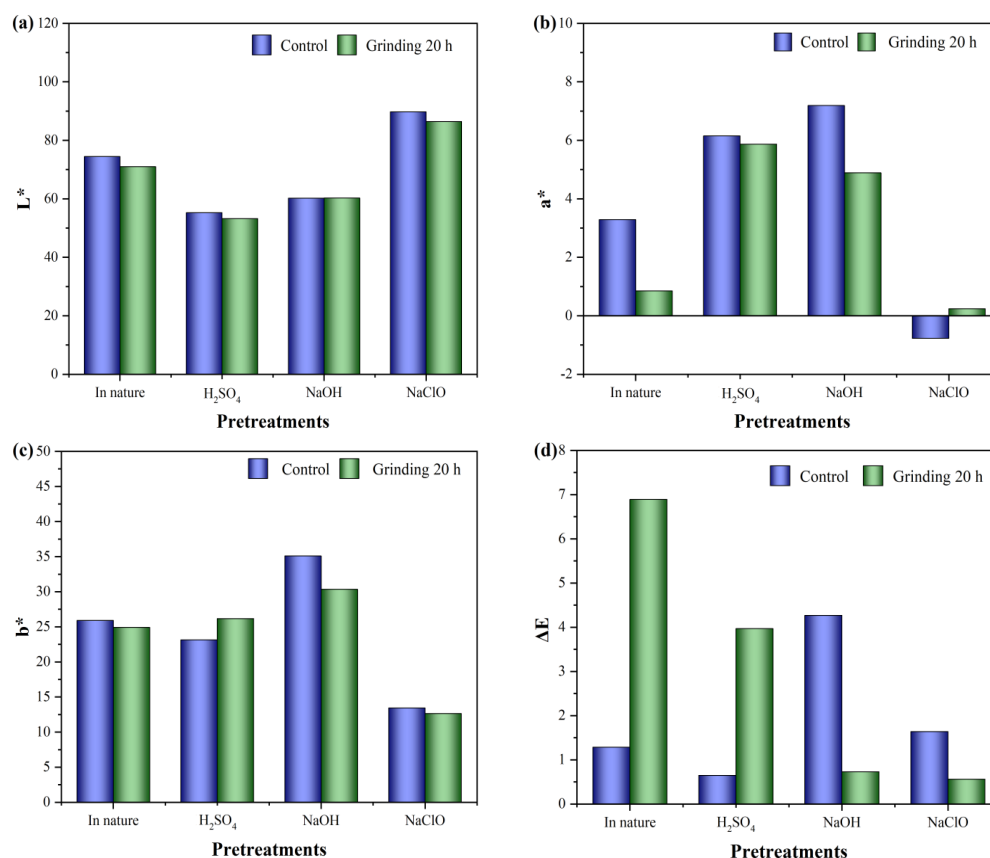


Figure 4. Colorimetric analysis (a) luminosity, (b) green-red coordinate, (c) blue-yellow coordinate, and (d) color variation.

3.3. Density Analysis

Figure 5 presents the density results for the *A. donax* L. samples. In an overall context, the results of this investigation revealed a consistent pattern of increasing biomass density as milling time was prolonged. This observation is consistent with a general trend in many particulate materials, where particle compaction leads to an increase in density. The rationale for this behavior can be attributed to the reduction in particle size during the milling process. As the particles are reduced in size, they have a larger surface area relative to their volume. Therefore, this leads to greater efficiency in packing the particles due to decreased space between them, consequently resulting in increased density [55]. Further-

more, it is observed that the in natura sample reached a higher density of 0.218 g/cm^3 after 20 h of milling compared to the pre-treated samples. Pretreatments can significantly influence the characteristics of the material, including its density, as they aim to extract specific components of the biomass, such as lignin, hemicellulose, and other undesirable compounds, thus affecting the density through mass reduction.

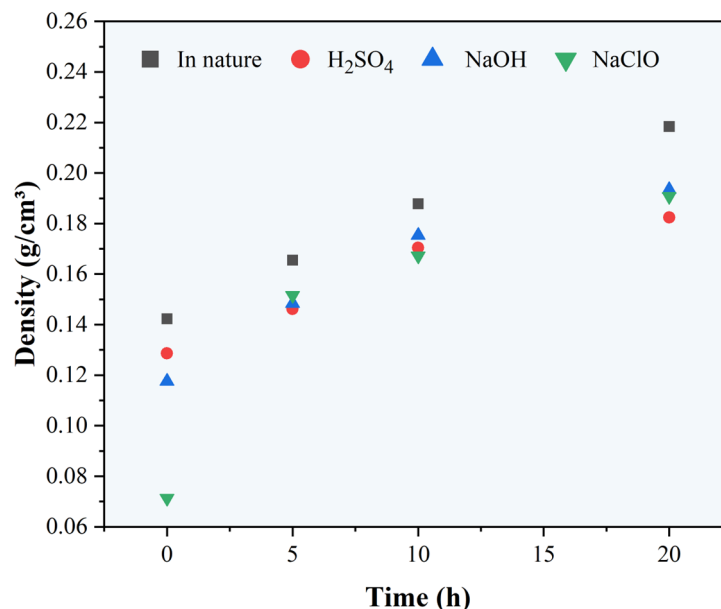


Figure 5. Density of *A. donax* L. samples in natura and chemically pretreated that were subjected to different milling times.

3.4. Particle Size Distribution

The particle size distribution obtained by laser diffraction is presented by the histograms in Figure 6 and Table 1. In general, the histograms present monomodal behavior, indicating a more uniform particle size distribution. However, in the samples pre-treated with NaClO for 10 h and 20 h of milling, two peaks appeared, indicating bimodal behavior, suggesting that milling under these conditions led to the formation of two distinct granulometric populations. Depending on the pretreatment conditions, intermediate products may form that affect the grinding and breakage of the particles, leading to the formation of two peaks. In some cases, during the grinding process, the particles may agglomerate or aggregate due to attractive forces between them [56–58]. In addition, moisture can play an important role in the grinding of materials. Variations in sample moisture content over the milling time can affect the particle size distribution, creating distinct peaks. Considerable variation in the mean particle diameter (D_m) was observed for the different pretreatments over the milling time.

The analysis of the particle size distribution of the In natura samples demonstrated a typical behavior of untreated lignocellulosic materials, with an initial D_m of $242.03 \mu\text{m}$ (control), characterized by a coarser structure. This broader particle size distribution can be attributed to the presence of lignin, cellulose and hemicellulose in their natural form, where lignin acts as a structural and reinforcing agent, limiting the physical manipulation of the fibers and, consequently, hindering fragmentation during the milling process. After 5 h of milling, a significant reduction in particle size was observed, resulting in a D_m of $96.73 \mu\text{m}$. This behavior can be explained by the partial defibrillation of lignin and hemicellulose during the mechanical process, which weakens the fibrous structure of the biomass.

Pretreatment with H_2SO_4 after 10 h of milling showed a smaller particle size of $49.92 \mu m$ compared to the in natura samples and the other chemical pretreatments. Although this pretreatment presents a higher lignin composition, which could act as a reinforcing agent, the chemical modification of the matrix occurs due to the chemical process with H_2SO_4 , causing a de-structuring of the biomass, making it more fragile and susceptible to fracture. Acid pretreatment can produce oxygenated functional groups, such as carbonyls and carboxyls, which contribute to lignin oxidation [59]. These new groups make lignin more reactive, facilitating the fragmentation of macromolecules. Therefore, acid treatment not only reduces lignin's resistance to particle breakage, which is relevant for subsequent processes such as comminution. This can be attributed to the fact that, although less lignin is removed in this process, sulfuric acid causes a destructuring of the biomass, making it more fragile and susceptible to fracture. This same behavior was reported by Sun and Cheng, 2005 [31].

In contrast, the samples pretreated with NaOH and NaClO presented a D_m of $79.01 \mu m$ and $76.74 \mu m$, respectively, evidencing a larger particle diameter after 20 h of milling. This behavior can be explained by changes in the chemical and physical properties resulting from the high concentration of cellulose and hemicellulose preserved in pretreatments with NaOH and NaClO. This composition provides greater resistance to particle breakage through the mechanical process. Siqueira et al. (2013) [46], who used NaOH as a pretreatment agent, showed that although sodium hydroxide is efficient in removing lignin, it better preserves cellulose structures, which can result in greater resistance to mobility.

Therefore, this study highlights the efficiency of milling, which depends not only on the removal of constituents, but also on the structural changes caused by the type of chemical pretreatment and milling time applied. The combination of chemical and physical pretreatment may enhance the dispersion of biomass constituents in the polymer matrix, a crucial factor for the development of high-performance films and composite materials.

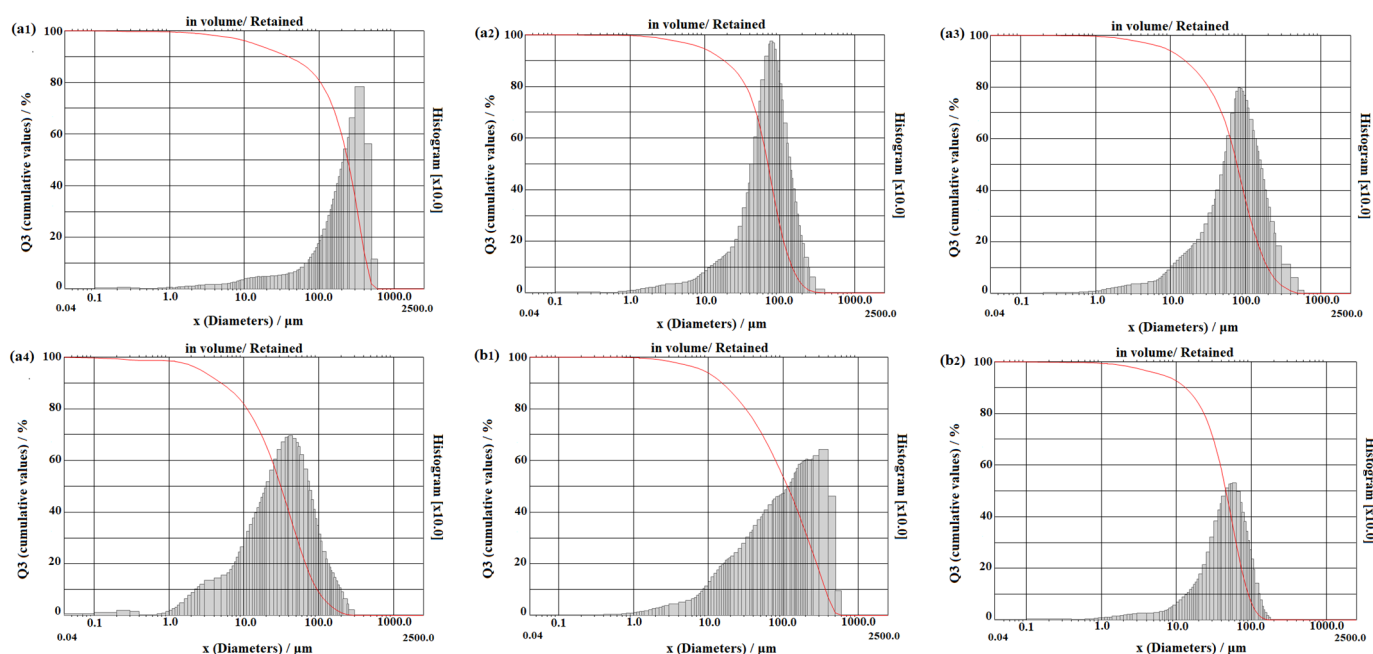


Figure 6. Cont.

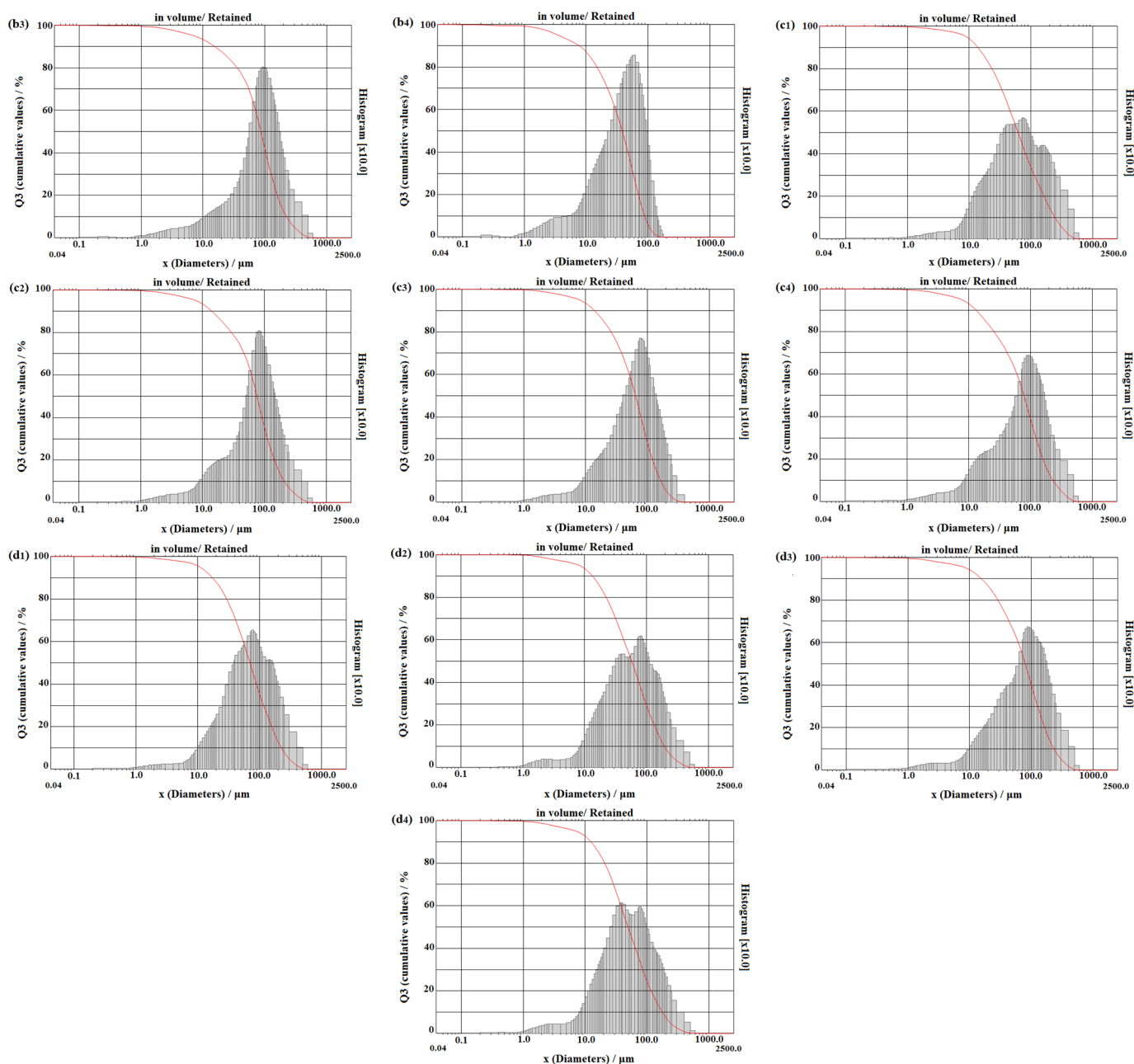


Figure 6. Particle size distribution of *A. donax* L. (a) in natura *in natura* and pretreated with: (b) H_2SO_4 , (c) NaOH, and (d) NaClO, where: (1) 0 h (control), (2) 5 h, (3) 10 h, and (4) 20 h.

Table 1. Particle size distribution.

Pretreatments	Grinding Time (h)	Particle Diameter (μm)			
		D ₁₀	D ₅₀	D ₉₀	D _m
in natura	control	38.33	241.59	432.43	242.03
	5	15.91	77.12	198.15	96.73
	10	18.07	69.67	147.16	78.59
	20	4.97	31.37	96.11	43.48
H_2SO_4	control	15.23	114.40	368.63	156.56
	5	15.38	86.57	224.96	108.60
	10	13.14	45.83	91.49	49.92
	20	7.71	38.49	89.20	44.31

Table 1. Cont.

Pretreatments	Grinding Time (h)	Particle Diameter (μm)			
		D ₁₀	D ₅₀	D ₉₀	D _m
NaOH	control	13.22	78.60	233.52	104.93
	5	13.81	62.32	246.33	100.43
	10	14.14	76.38	210.59	99.40
	20	13.97	64.47	165.11	79.01
NaClO	control	15.50	79.92	233.95	106.37
	5	17.37	70.32	226.92	100.86
	10	13.39	57.75	195.35	85.98
	20	12.45	49.26	177.00	76.74

D_m : Average diameter; D_X : diameter where X% is below the presented particle size value.

3.5. Morphological Analysis

Figure 7 shows the morphological images resulting from the scanning electron microscopy (SEM) analysis of *A. donax* L. subjected to different chemical pretreatments and milling times. When comparing the particle size before and after the final milling period, a reduction in size and change in particle shape was evident in both the in natura and chemically pretreated samples, characterized by the presence of elongated and thin particles.

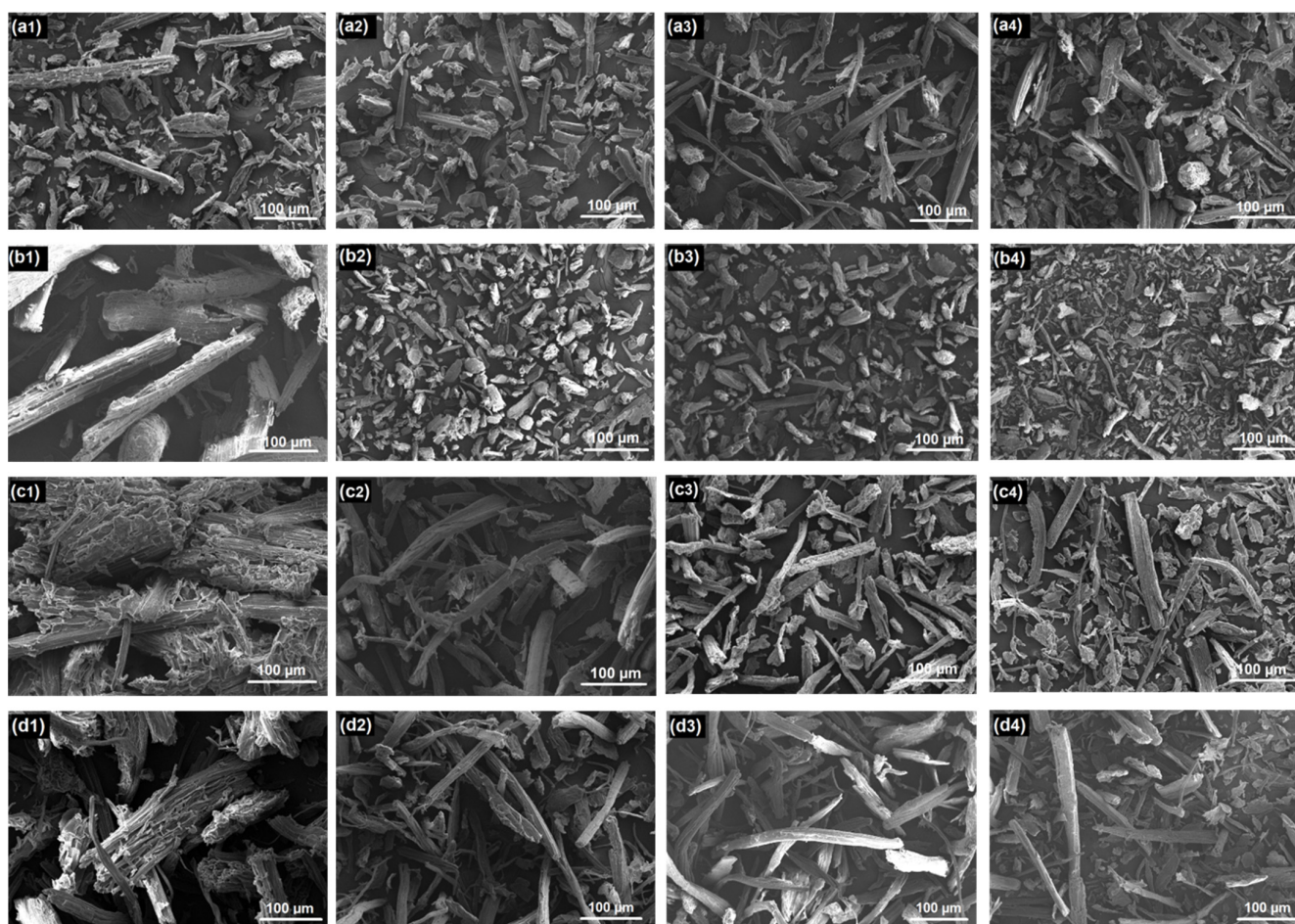


Figure 7. SEM analysis for *A. donax* L. (a) in natura, pretreated with: (b) H₂SO₄, (c) NaOH, and (d) NaClO; where: (1) 0 h (control), (2) 5 h, (3) 10 h, and (4) 20 h.

Rajaonarivony et al. (2023) [60] reported that a comminution friction mechanism tends to produce a more elongated mean shape than an impact mechanism. This observation suggests that the particle surface was defibrillated during the grinding process, due to

friction between the *A. donax* L. granules, the grinding balls, and the cylinder wall [61]. This phenomenon can be attributed to the increase in surface area, formation of cracks, and increased porosity during the milling process [62,63].

It is noted that pretreatment with H_2SO_4 resulted in the greatest structural changes, and it is evident that acid treatment was the most aggressive in terms of degradation of the biomass structure. This behavior is in line with the observations of the particle size distribution analysis (Section 3.4), which showed rapidly disintegrated fibers due to the combined effect of acid treatment and milling.

All samples showed that both grinding time and biomass type had a significant influence on particle size, with smaller sizes being observed after 20 h of grinding. Grinding demonstrated a positive impact on improving the particle size distribution of the biomass processed during this period, corroborating findings from other studies [64]. Therefore, a thorough understanding of the variables involved and the application of techniques to optimize particle size are essential to advance the production of lignocellulosic films. This optimization not only improves the quality of the final products but also enhances the viability of their applications in various industries, resulting in more resistant and uniform films.

3.6. Thermal Analysis

The investigation of the thermal properties of *A. donax* L. after chemical pretreatments and milling processes is of paramount importance, as it allows the determination of the maximum operating temperature for each condition without inducing thermal decomposition of the material. In this sense, Figure 8 presents the thermogravimetric analysis (TGA) and the derived thermogravimetric analysis (DTG), while Table S1 provides the percentage of mass loss.

In general, the thermogravimetric curves showed three stages of accentuated degradation, where the first stage represents the initial mass loss between 80 °C and 100 °C, which corresponds to the elimination of water (sample moisture); the second stage, also called the main stage, between 200 °C and 350 °C, which corresponds to the greatest mass loss of the lignocellulosic components; and the third stage, between 430 °C and 750 °C, which represents the residual mass loss of the components. According to Sathasivam e Haris, 2012 [65], in the decomposition of lignocellulosic materials, hemicellulose decomposes between 220 °C and 315 °C and cellulose between 315 °C and 400 °C and lignin, because it has a more complex structure, its range is between 150 °C and 800 °C.

Figure 8a shows the results obtained for the in natura sample. In the main degradation stage, a mass loss of 53.62% was observed for the control compared to the loss of 45.59% after 20 h of milling, a difference of 7.93% in the reduction in mass loss. This behavior may be related to the partial removal of volatile compounds and a possible reduction in hemicellulose and lignin. The partial removal of these components alters the structure of the biomass, making it more thermally unstable.

In Figure 8c, the results for the sample pretreated with H_2SO_4 revealed a mass loss of 58.74% (control) and a loss of 65.10% after 10 h of milling, resulting in an increase in the difference of 6.36%. This behavior is related to the acid process and milling, which modify the lignin structure and reduce the particle size. This decrease in particle size increases the surface area, making the material more susceptible to thermal degradation.

Likewise, it is noted that for the sample pretreated with NaOH shown in Figure 8e, there was a mass loss of 38.43% (control) and 48.18% after 10 h of milling, an increase in the difference of 9.75%. NaOH, being an alkaline agent, is efficient in solubilizing lignin and hemicellulose, which results in a higher concentration of cellulose in the samples and, consequently, a greater mass loss at the temperatures corresponding to cellulose handling.

In Figure 8g the highest mass loss of 66.40% was observed for the sample pretreated with NaClO and milled for 10 h. This increase in mass loss may be related to the partial

removal of non-cellulosic components due to chemical pretreatment. According to Fischer et al., 2002 [66], the thermal behavior of lignocellulosic materials is related to their chemical composition and crystallinity. According to Kabir et al., (2012) [67], chemical pretreatment and treatment conditions also influence temperature and increase degradation loss, which can eventually weaken the material structure and damage it, impairing its thermal and mechanical properties. Therefore, it is noted that among the different pretreatments studied in this work, the highest mass losses were observed for those pretreated with H_2SO_4 and $NaClO$ after 10 h of milling, 65.10% and 66.40%, respectively, due to the partial removal of non-cellulosic components, and confirmed in chemical analyses.

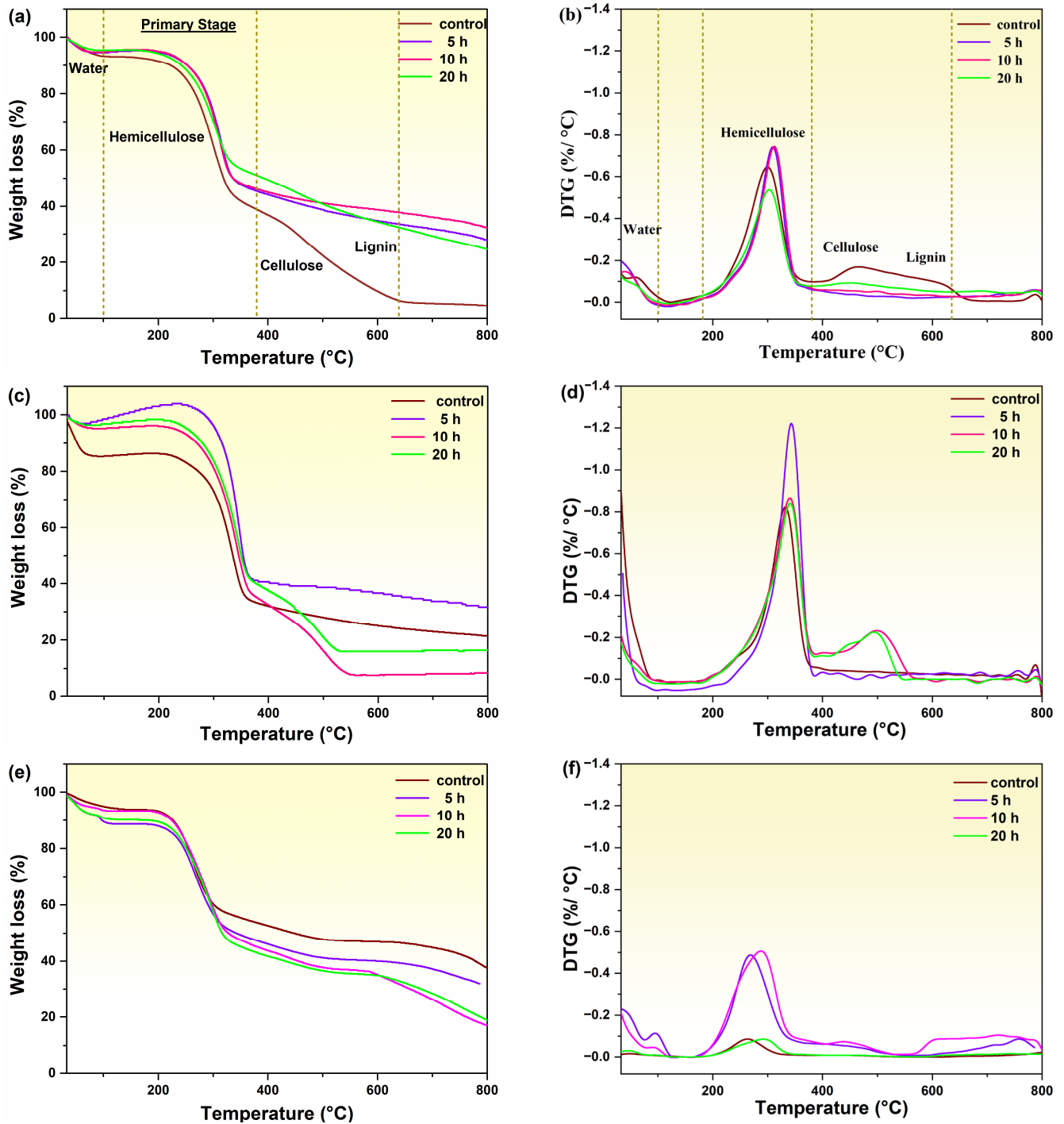


Figure 8. Cont.

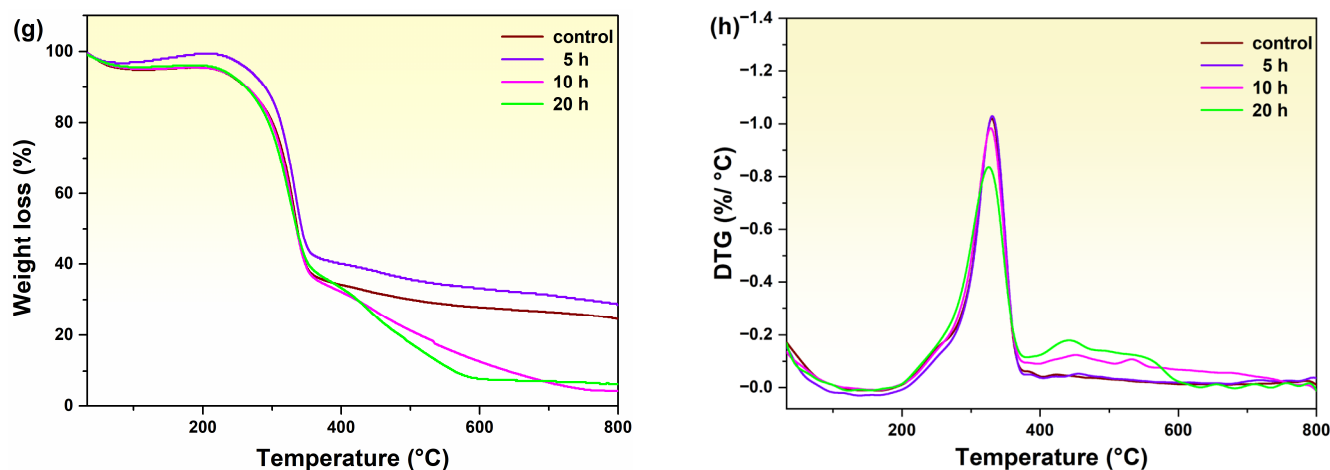


Figure 8. TG and DTG curve of *A. donax* L. (a–b) in natura; and pretreated with: (c–d) H_2SO_4 ; (e–f) NaOH , and (g–h) NaClO , 0 h (control), 5, 10, and 20 h of milling.

Another relevant fact is shown in Table S1 with the initial and final temperatures (T_{start} and T_{end}) of the main degradation stages of the chemical pretreatments. According to Elango et al., (2023) [68], as the non-crystalline character of the material decreases, there is a shift in the maximum degradation temperature, which will occur at a higher temperature, since the non-crystalline regions are more active in relation to the crystalline against thermal decomposition. This fact can be evidenced by comparing the temperatures of the in natura sample (non-crystalline character) before (control) and after 20 h of milling (T_{start} 256.50 °C and T_{end} 325.92 °C), with the sample pretreated with NaClO (crystalline character) for 10 h of milling (T_{start} 292.96 °C and T_{end} 345.13 °C). The crystalline character of *A. donax* L. is in agreement with the results obtained in the X-ray diffraction analyses.

Furthermore, the increase in milling time also altered the thermal properties of chemically pretreated *A. donax*. For all pretreatments, the greatest mass loss was evident after 10 h of milling. Therefore, this behavior can be explained by the defibrillation of the particles by the mechanical milling process, altering their particle size and consequently increasing their surface area, as can be observed in the SEM analyses.

In the DTG curves, two intense peaks are observed, the first being characterized by the decomposition of hemicellulose and degradation of the crystalline structure of cellulose (main stage), and the second peak corresponding to the degradation of lignin (secondary stage). Furthermore, a greater intensity of this peak is noted for those pretreated with H_2SO_4 (Figure 8d) after 5 h of milling and pretreated with NaClO (Figure 8h) after 10 and 20 h. According to Monteiro et al., 2013 [69], this behavior is attributed to the presence of lignin and hemicellulose compounds in its composition.

3.7. FT-IR Analysis

FT-IR was used to investigate the chemical changes resulting from the different pretreatment methods. Figure 9 shows the FT-IR spectra obtained for the different samples. In general, the spectra present an intense peak at 3340 cm^{-1} that may be related to the stretching vibrations of the hydroxyl groups of the cellulose and lignin molecules [70]. Although a considerable portion of lignin is removed by the applied treatments, the $-\text{OH}$ signals in the spectra remain practically unchanged due to the high cellulose content in all the samples. The peak at $\sim 1740\text{ cm}^{-1}$ is attributed to carbonyl stretching of acetyl groups in hemicellulose and alpha-keto carboxylic acid in lignin. An additional and less significant peak is found in the feedstock at $\sim 1240\text{ cm}^{-1}$, which may be related to CO bonding in hemicelluloses [71].

In Figure 9a, the samples subjected to H_2SO_4 pretreatment exhibit a distinct feature characterized by an increased intensity in the absorption band at 3340 cm^{-1} compared to other pretreatment methods. This variation suggests a possible change in the hydrophilicity of the material due to the reduction of hydroxyl groups caused by other chemical pretreatments, subsequently leading to a reduction in water absorption. Furthermore, a notable change can be observed at $\sim 1595\text{ cm}^{-1}$, attributed to the axial deformation of the $\text{C}=\text{C}$ bonds within the aromatic rings of lignin [72]. This change is characterized by a decrease in peak intensity for samples treated with NaOH and NaClO . This decrease provides evidence that these specific chemical pretreatments did not completely remove lignin and hemicellulose from the analyzed material. This observation is consistent with the results of the chemical characterizations performed in this study.

Comparing the spectra in Figure 9a,b, a certain similarity is apparent; however, there is a reduction in the intensity of the peak at $\sim 1464\text{ cm}^{-1}$ for the NaOH -treated sample. Similarly, the peaks at 3340 and 1688 cm^{-1} for the H_2SO_4 -treated samples also show decreased intensity. These results collectively indicate that the milling process does not induce significant changes in the chemical properties of the material. Therefore, it can be attributed to deformation or bond breaking [73], which corroborates the results presented in Section 3.4.

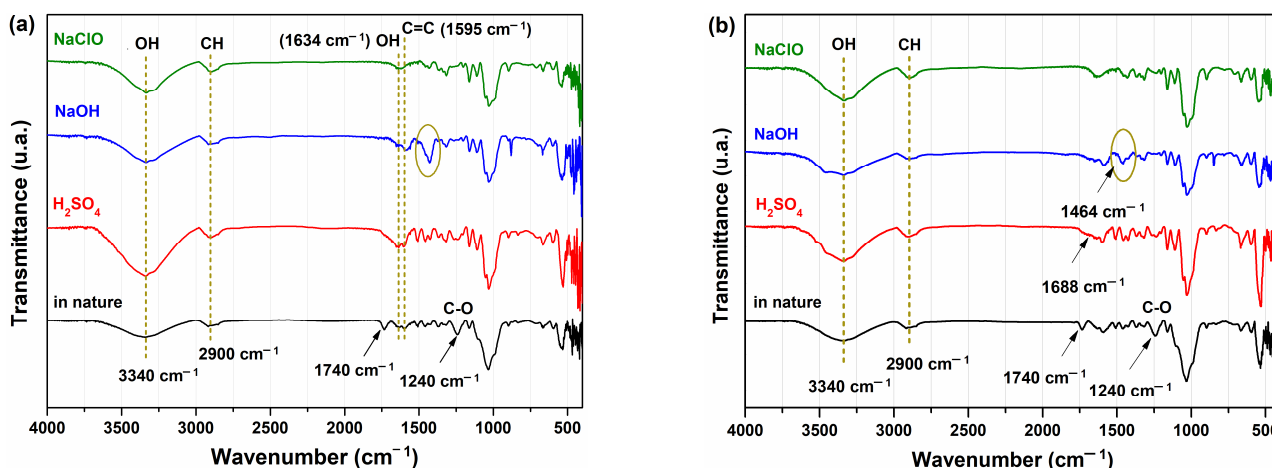


Figure 9. FT-IR analysis of *A. donax* L. (a) 0 h (control) and (b) 20 h of milling.

3.8. XRD Analysis

The XRD technique was applied to investigate the presence of crystalline regions in *A. donax* L. samples before (control) and after 20 h of milling. In general, the diffractograms in Figure 10 exhibit three main peaks, with two more prominent peaks at approximately 15° (110) and 22° (200), followed by a less intense peak at 34° (004). These characteristic diffraction peaks are typical patterns associated with cellulose [74,75].

Figure 10a shows the diffractograms for the in natura sample. It is noticeable that after 20 h of grinding, there is a reduction in the intensity of the largest peaks in relation to the other grinding times. This phenomenon suggests that prolonged grinding induces exfoliation and partial rupture of the crystalline region of cellulose due to friction between the *A. donax* L. particles, the grinding balls and the walls of the jar. Consequently, this exposes a greater number of hydroxyl groups, which is in agreement with FT-IR analyses. Samples pretreated with H_2SO_4 aim to isolate the (insoluble) lignin, thus removing the holocellulose (hemicellulose and cellulose).

Although lignin is an amorphous polymer with a three-dimensional structure, the sample pretreated with H_2SO_4 exhibited peaks in the diffractograms, illustrated in Figure 10b, with similar behavior to that of the in natura sample, but with higher peak intensities.

This increase in peak intensity can be attributed to the partial removal of extractives and hemicelluloses, which leads to the reduction in the amorphous portion of the structure, but mainly due to the high content of cellulose remaining in the samples (as evidenced by chemical characterization).

The samples pretreated with NaOH (Figure 10c) and NaClO (Figure 10d) exhibited behavior consistent with the diffraction patterns, corresponding to the cellulose peaks. This pattern can be attributed to the higher cellulose content associated with these pretreatment methods compared to the previous ones. Table 2 clearly shows that the crystallinity of chemically pretreated *A. donax* L. samples depends on the grinding time, which probably improves the surface area and increases their amorphism. The lowest crystallinity, of 17.43%, was observed for the sample pretreated with H₂SO₄ during 20 h of milling. The results presented attest that the crystallinity decreases with the increase in milling time.

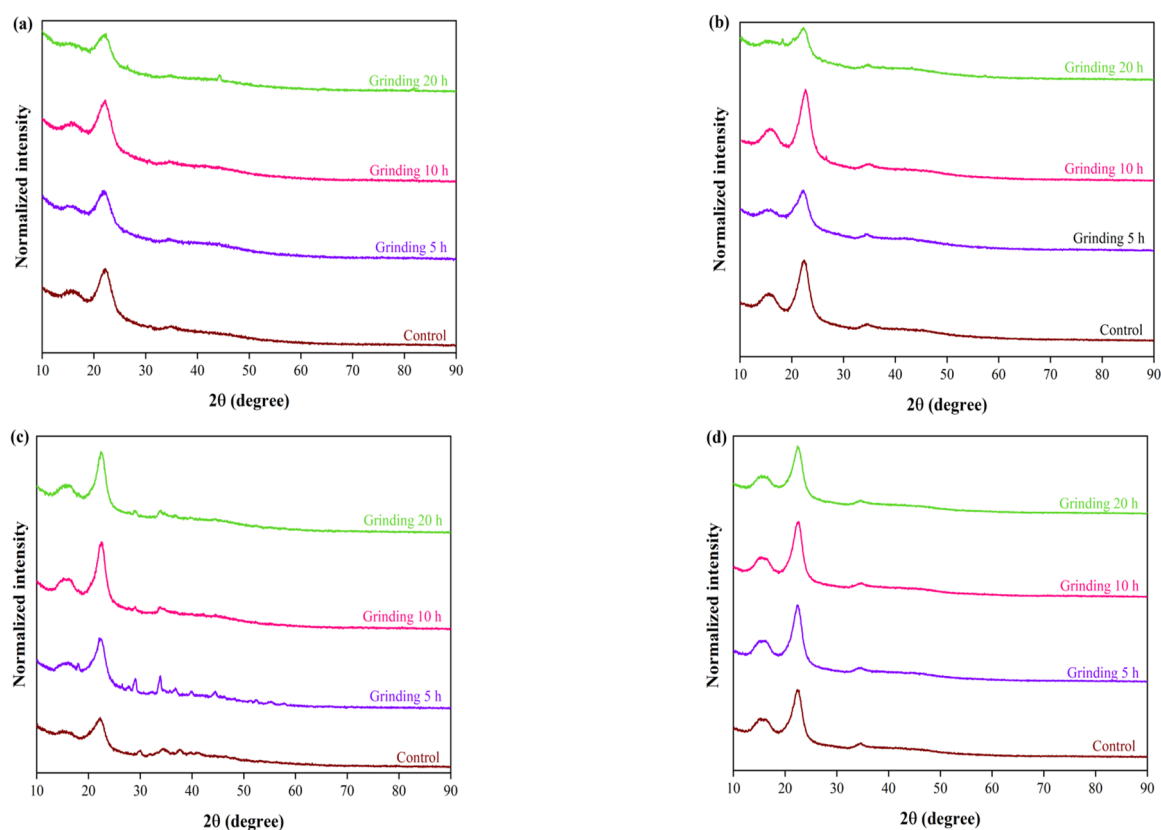


Figure 10. XRD analysis of *A. donax* L. (a) in natura; and pretreated with: (b) H₂SO₄; (c) NaOH, and (d) NaClO, 0 h (control), 5, 10, and 20 h of milling.

Table 2. Average crystallinity index of the samples.

Pretreatments	IC%			
	Control	5 h	10 h	20 h
in natura	23.24	21.80	23.03	19.52
H ₂ SO ₄	35.81	19.05	33.63	17.43
NaOH	28.05	28.09	29.92	24.73
NaClO	33.39	37.04	30.04	30.76

4. Conclusions

This study demonstrates that the combination of chemical and physical pretreatments is an innovative and effective approach for the modification of *Arundo donax* L. biomass,

making it promising for the future production of high-quality and high-performance biodegradable materials. Pretreatment with NaClO was the most efficient in terms of lignin removal and cellulose preservation, resulting in a high cellulose content (67%). This suggests greater efficiency in the formation of homogeneous materials for biodegradable packaging applications. In addition, the samples pretreated with NaClO showed bimodal behavior in the particle size distribution at milling times of 10 and 20 h. Pretreatment with H₂SO₄, although resulting in a high residual lignin content (24%), was effective in reducing the average particle diameter to 44.31 μm.

In addition, the study innovates by correlating the effects of pretreatment and milling with critical parameters, such as thermal stability, density, and morphological changes. The observed improvements in thermal properties, with a mass loss of 66.4% for NaClO-treated samples, highlight the role of combined processes in modifying material resilience and performance. Morphological analysis revealed distinct structural transformations, such as defibrillation and the formation of elongated particles, which are critical for the development of biodegradable films and composite materials.

Supplementary Materials: The following supporting information can be downloaded at: <https://docs.google.com/document/d/14SEbLIZGslv4tsYUhfETNz0kdym5cyDp/edit?usp=sharing&oid=106537514886602130224&rtfpof=true&sd=true>, Table S1: Values obtained by thermogravimetric analyzes.

Author Contributions: P.O.S.: Conceptualization, validation, formal analysis, investigation, writing—original draft preparation, writing—review and editing, visualization, supervision, project administration; D.d.S.R.: Methodology, formal analysis, investigation, writing—original draft preparation; M.d.P.G.: Methodology, formal analysis, investigation, writing—original draft preparation; S.H.F.d.S.: Methodology, formal analysis, investigation, writing—original draft preparation; M.M.M.: formal analysis, investigation, writing—original draft preparation; D.A.G.: Validation, resources; C.F.L.e.S.: Validation, resources; C.M.C.: Conceptualization, validation, resources, writing—original draft preparation, writing—review and editing; A.L.M.: Conceptualization, validation, resources, writing—original draft preparation, writing—review and editing, visualization, supervision, project administration. All authors have read and agreed to the published version of the manuscript.

Funding: The authors are indebted to Fundação de Amparo à Pesquisa do Estado de Rio Grande do Sul (FAPERGS, grant 21/2551-0000603-0), the Brazilian National Council for Scientific and Technological Development (CNPq, grants 408118/2023-7 and 311975/2023-2), and Coordination for the Improvement of Higher Education Personnel—Brazil (Capes, grant 001) for the financial support given to this research.

Data Availability Statement: The original contributions presented in the study are included in the article/Supplementary Material. Further inquiries can be directed to the corresponding author/s.

Acknowledgments: The authors thank the Brazilian Agricultural Research Corporation (EMBRAPA) for donating the raw material.

Conflicts of Interest: The authors declare no competing interests.

References

1. Al-Snafi, A.E. The constituents and biological effects of *Arundo donax*—A review. *Int. J. Phytopharm. Res.* **2017**, *6*, 34–40.
2. Antal, G. Giant reed (*Arundo donax* L.) from ornamental plant to dedicated bioenergy species: Review of economic prospects of biomass production and utilization. *Int. J. Hortic. Sci.* **2018**, *24*, 39–46. [CrossRef]
3. Ortega, Z.; Bolaji, I.; Suárez, L.; Cunningham, E. A review of the use of giant reed (*Arundo donax* L.) in the biorefineries context. *Rev. Chem. Eng.* **2024**, *40*, 305–328. [CrossRef]
4. Shatalov, A.A.; Pereira, H. Papermaking fibers from giant reed (*Arundo donax* L.) by advanced ecologically friendly pulping and bleaching technologies. *BioResources* **2006**, *1*, 45–61. [CrossRef]
5. Molari, L.; Coppolino, F.S.; García, J.J. *Arundo donax*: A widespread plant with great potential as sustainable structural material. *Constr. Build. Mater.* **2021**, *268*, 121143. [CrossRef]

6. Garcez, L.P.R.; Gatti, T.F.; Gonzalez, J.C.; Franco, A.C.; Ferreira, C.S. Characterization of Fibers from Culms and Leaves of *Arundo donax* L. (*Poaceae*) for Handmade Paper Production. *J. Nat. Fibers* **2022**, *19*, 12805–12813. [CrossRef]
7. Dell’omo, P.P.; Spina, V.A. Mechanical pretreatment of lignocellulosic biomass to improve biogas production: Comparison of results for giant reed and wheat straw. *Energy* **2020**, *203*, 117798. [CrossRef]
8. Corno, L.; Pili, R.; Adani, F. *Arundo donax* L.: A non-food crop for bioenergy and bio-compound production. *Biotechnol. Adv.* **2014**, *32*, 1535–1549. [CrossRef]
9. Mesa, L.; Martínez, Y.; Barrio, E.; González, E. Desirability function for optimization of Dilute Acid pretreatment of sugarcane straw for ethanol production and preliminary economic analysis based in three fermentation configurations. *Appl. Energy* **2017**, *198*, 299–311. [CrossRef]
10. Ferrarini, A.; Fracasso, A.; Spini, G.; Fornasier, F.; Taskin, E.; Fontanella, M.C.; Beone, G.M.; Amaducci, S.; Puglisi, E. Bioaugmented Phytoremediation of Metal-Contaminated Soils and Sediments by Hemp and Giant Reed. *Front. Microbiol.* **2021**, *12*, 645893. [CrossRef]
11. Amaducci, S.; Perego, A. Field evaluation of *Arundo donax* clones for bioenergy production. *Ind. Crops Prod.* **2015**, *75*, 122–128. [CrossRef]
12. De Bari, I.; Liuzzi, F.; Ambrico, A.; Trupo, M. *Arundo donax* Refining to Second Generation Bioethanol and Furfural. *Processes* **2020**, *8*, 1591. [CrossRef]
13. Martínez-Sanz, M.; Erboz, E.; Fontes, C.; López-Rubio, A. Valorization of *Arundo donax* for the production of high performance lignocellulosic films. *Carbohydr. Polym.* **2018**, *199*, 276–285. [CrossRef]
14. Araújo, D.; Vilarinho, M.; Machado, A. Effect of combined dilute-alkaline and green pretreatments on corncob fractionation: Pretreated biomass characterization and regenerated cellulose film production. *Ind. Crops Prod.* **2019**, *141*, 111785. [CrossRef]
15. Niu, L.; Guo, Q.; Xiao, J.; Li, Y.; Deng, X.; Sun, T.; Liu, X.; Xiao, C. The effect of ball milling on the structure, physicochemical and functional properties of insoluble dietary fiber from three grain bran. *Food Res. Int.* **2023**, *163*, 112263. [CrossRef]
16. Li, J.; Yang, Z.; Zhang, K.; Liu, M.; Liu, D.; Yan, X.; Si, M.; Shi, Y. Valorizing waste liquor from dilute acid pretreatment of lignocellulosic biomass by *Bacillus megaterium* B-10. *Ind. Crops Prod.* **2021**, *161*, 113160. [CrossRef]
17. Woiciechowski, A.L.; Neto, C.J.D.; de Souza Vandenberghe, L.P.; de Carvalho Neto, D.P.; Sydney, A.C.N.; Letti, L.A., Jr.; Karp, S.G.; Torres, L.A.Z.; Soccol, C.R. Lignocellulosic biomass: Acid and alkaline pretreatments and their effects on biomass recalcitrance—Conventional processing and recent advances. *Bioresour. Technol.* **2020**, *304*, 122848. [CrossRef]
18. Smits, J.; van Haastert, M.; Janse, A.M.C.; Maas, J.; de Graaf, K.; Kroon, H.; Verlinden, R.A.; Happel, A. Scale-up of optimal mild-acid pretreatment conditions in the production and application of lignocellulosic sugars from wood. *Bioresour. Technol. Rep.* **2020**, *9*, 100361. [CrossRef]
19. Lemões, J.S.; e Silva, C.F.L.; Avila, S.P.F.; Montero, C.R.S.; Silva, S.D.d.A.e.; Samios, D.; Peralba, M.D.C.R. Chemical pretreatment of *Arundo donax* L. for second-generation ethanol production. *Electron. J. Biotechnol.* **2018**, *31*, 67–74. [CrossRef]
20. Kim, J.S.; Lee, Y.Y.; Kim, T.H. A review on alkaline pretreatment technology for bioconversion of lignocellulosic biomass. *Bioresour. Technol.* **2016**, *199*, 42–48. [CrossRef]
21. Park, Y.C.; Kim, J.S. Comparison of various alkaline pretreatment methods of lignocellulosic biomass. *Energy* **2012**, *47*, 31–35. [CrossRef]
22. Bajpai, P. Pulp Bleaching. In *Biermann’s Handbook of Pulp and Paper*; Elsevier: New York, NY, USA, 2018; pp. 465–491.
23. Vasileiadou, A. From Organic Wastes to Bioenergy, Biofuels, and Value-Added Products for Urban Sustainability and Circular Economy: A Review. *Urban. Sci.* **2024**, *8*, 121. [CrossRef]
24. Yang, C.; Yuan, X.; Wang, X.; Wu, K.; Liu, Y.; Liu, C.; Lu, H.; Liang, B. Ball milling promoted direct liquefaction of lignocellulosic biomass in supercritical ethanol. *Front. Chem. Sci. Eng.* **2020**, *14*, 605–613. [CrossRef]
25. Zhai, Q.; Li, F.; Wang, F.; Feng, J.; Jiang, J.; Xu, J. Ultrafine grinding of poplar biomass: Effect of particle morphology on the liquefaction of biomass for methyl glycosides and phenolics. *Cellulose* **2019**, *26*, 3685–3701. [CrossRef]
26. Ewulonu, C.M.; Liu, X.; Wu, M.; Huang, Y. Ultrasound-assisted mild sulphuric acid ball milling preparation of lignocellulose nanofibers (LCNFs) from sunflower stalks (SFS). *Cellulose* **2019**, *26*, 4371–4389. [CrossRef]
27. Deng, S.; Huang, R.; Zhou, M.; Chen, F.; Fu, Q. Hydrophobic cellulose films with excellent strength and toughness via ball milling activated acylation of microfibrillated cellulose. *Carbohydr. Polym.* **2016**, *154*, 129–138. [CrossRef]
28. Krička, T.; Matin, A.; Bilandžija, N.; Jurišić, V.; Antonović, A.; Voča, N.; Grubor, M. Biomass valorisation of *Arundo donax* L., *Miscanthus × giganteus* and *Sida hermaphrodita* for biofuel production. *Int. Agrophysics* **2017**, *31*, 575–581. [CrossRef]
29. Fiore, V.; Botta, L.; Scaffaro, R.; Valenza, A.; Pirrotta, A. PLA based biocomposites reinforced with *Arundo donax* fillers. *Compos. Sci. Technol.* **2014**, *105*, 110–117. [CrossRef]
30. United Nations. Sustainable Development Goals (SDG) Report. Available online: <https://unstats.un.org/sdgs/report/2021/Overview/> (accessed on 18 February 2024).
31. Sun, Y.; Cheng, J.J. Dilute acid pretreatment of rye straw and bermudagrass for ethanol production. *Bioresour. Technol.* **2005**, *96*, 1599–1606. [CrossRef]

32. Nascimento, V.M.; Manrich, A.; Tardioli, P.W.; de Campos Giordano, R.; de Moraes Rocha, G.J.; Giordano, R.d.L.C. Alkaline pretreatment for practicable production of ethanol and xylooligosaccharides. *Bioethanol* **2016**, *2*. [[CrossRef](#)]
33. Wijaya, C.J.; Ismadji, S.; Aparamarta, H.W.; Gunawan, S. Optimization of cellulose nanocrystals from bamboo shoots using Response Surface Methodology. *Heliyon* **2019**, *5*, e02807. [[CrossRef](#)] [[PubMed](#)]
34. Standard T, Standard O, Method C, Practice S, The T. T 257 sp-12. 2012. TAPPI. (2012). *Sampling and preparing wood for analysis (T 257 sp-12)*. Technical Association of the Pulp and Paper Industry.
35. Tappi T 222 om-11 (1). TAPPI Press: Atlant, GA, USA, 2011. Technical Association of the Pulp and Paper Industry Acid-Insoluble Lignin in Wood and Pulp. Available online: <https://imisrise.tappi.org/TAPPI/Products/01/T/0104T222.aspx> (accessed on 14 January 2025).
36. Mashalavi, B. Investigation of UV shielding of bio-based superhydrophobic outdoor wood paint properties. *Res. Sq.* **2024**, 1–18.
37. Acosta, A.P.; Barbosa, K.T.; Amico, S.C.; Missio, A.L.; Delucis, R.d.A.; Gatto, D.A. Improvement in mechanical, physical and biological properties of eucalyptus and pine woods by raw pine resin in situ polymerization. *Ind. Crops Prod.* **2021**, *166*, 113495. [[CrossRef](#)]
38. Smits, M.; Kronbergs, E. Density determination for biomass compositions. *Eng. Rural. Dev.* **2012**, *11*, 300–303.
39. Ribeiro, A.C.R.; Rodrigues, M.B.B.; Ribes, D.D.; Cholant, C.M.; Lima, G.d.S.; Valim, G.C.; Delucis, R.d.A.; de Oliveira, A.D.; Carreño, N.L.V.; Gatto, D.A.; et al. Effect of xanthan gum on the physical and chemical features of microfibrillated cellulose films plasticized by glycerol. *Biomass Convers. Biorefinery* **2024**, *14*, 22203–22214. [[CrossRef](#)]
40. ASTM E1131-20; Standard Test Method for Compositional Analysis by Thermogravimetry. ASTM International: West Conshohocken, PA, USA, 2014.
41. Spectrometers, D.I.; Performance, M.; Tests, L.O. Standard Practice for iTeh Standards iTeh Standards Document Preview. **2021**, *98*, 1–7. American Society for Testing and Materials Standard Practice for General Techniques for Obtaining Infrared Spectra for Qualitative Analysis. Available online: <http://www.astm.org/cgi-bin/resolver.cgi?E1252-98R21> (accessed on 14 January 2025).
42. Taherzadeh, M.J.; Karimi, K. Acid-based hydrolysis processes for ethanol from lignocellulosic materials: A Review. *Bioethanol review*. *BioResources* **2007**, *2*, 472–499. [[CrossRef](#)]
43. Zhang, X.; Tanguy, N.R.; Chen, H.; Zhao, Y.; Gnanasekar, P.; Le Lagadec, R.; Yan, N. Lignocellulosic nanofibrils as multifunctional component for high-performance packaging applications. *Mater. Today Commun.* **2022**, *31*, 103630. [[CrossRef](#)]
44. Bian, H.; Chen, L.; Dai, H.; Zhu, J. Integrated production of lignin containing cellulose nanocrystals (LCNC) and nanofibrils (LCNF) using an easily recyclable di-carboxylic acid. *Carbohydr. Polym.* **2017**, *167*, 167–176. [[CrossRef](#)]
45. Chen, J.L.; Zhao, Y. Effect of Molecular Weight, Acid, and Plasticizer on the Physicochemical and Antibacterial Properties of β -Chitosan Based Films. *J. Food Sci.* **2012**, *77*, 127–136. [[CrossRef](#)]
46. Siqueira, G.; Várnai, A.; Ferraz, A.; Milagres, A.M. Enhancement of cellulose hydrolysis in sugarcane bagasse by the selective removal of lignin with sodium chlorite. *Appl. Energy* **2013**, *102*, 399–402. [[CrossRef](#)]
47. Zhao, J.; Dong, Z.; Li, J.; Chen, L.; Bai, Y.; Jia, Y.; Shao, T. Ensiling as pretreatment of rice straw: The effect of hemicellulase and *Lactobacillus plantarum* on hemicellulose degradation and cellulose conversion. *Bioresour. Technol.* **2018**, *266*, 158–165. [[CrossRef](#)] [[PubMed](#)]
48. Devarajan, A.; Markutsya, S.; Lamm, M.H.; Cheng, X.; Smith, J.C.; Baluyut, J.Y.; Kholod, Y.; Gordon, M.S.; Windus, T.L. Ab Initio Study of Molecular Interactions in Cellulose I α . *J. Phys. Chem. B* **2013**, *117*, 10430–10443. [[CrossRef](#)] [[PubMed](#)]
49. Ching, Y.C.; Ng, T.S. Effect of Preparation Conditions on Cellulose from Oil Palm Empty Fruit Bunch Fiber. *BioResources* **2014**, *9*, 6373–6385. [[CrossRef](#)]
50. de Melo, L.M.; Fernandes, L.N.; Soares, M.G.; Schmidt, V.C.R.; de Lima, M. Perspectivas no aproveitamento de resíduos agroindustriais ricos em celulose para o desenvolvimento de biopolímeros comestíveis. *Rev. Perspect.* **2023**, *47*, 117–132.
51. Pandian, B.; Ramalingam, S.; Sreeram, K.J.; Rao, J.R. Natural pigment: Preparation of brown pigment from lignin biomass for coloring application. *Dyes Pigment.* **2021**, *195*, 109704. [[CrossRef](#)]
52. Camargo, S.K.D.C.A.; Ventorim, G.; Camargo, B.S.; Salvador, R.; De Carvalho Araújo, C.K.; De Carvalho Araújo, C.K.C.; Henrique Antunes Vieira, F. Proposal for the conversion of *Eucalyptus urograndis* into bioethanol via acid hydrolysis, using the concepts of biorefineries. *Nord. Pulp. Pap. Res. J.* **2022**, *37*, 576–585. [[CrossRef](#)]
53. Delucis, R.D.A.; Beltrame, R.; Gatto, D.A. Discolouration of heat-treated fast-growing eucalyptus wood exposed to natural weathering. *Cellul. Chem. Technol.* **2019**, *53*, 635–641. [[CrossRef](#)]
54. Acosta, A.P.; Schulz, H.R.; Barbosa, K.T.; Zanol, G.S.; Gallio, E.; Delucis, R.d.A.; Gatto, D.A. Dimensional stability and colour responses of *Pinus Elliottii* wood subjected to furfurylation treatments. *Maderas-Cienc. Tecnol.* **2020**, *22*, 303–310. [[CrossRef](#)]
55. Olhero, S.M.; Ferreira, J.M.F. Influence of particle size distribution on rheology and particle packing of silica-based suspensions. *Powder Technol.* **2004**, *139*, 69–75. [[CrossRef](#)]
56. Forsyth, A.J.; Rhodes, M.J. A Simple Model Incorporating the Effects of Deformation and Asperities into the van der Waals Force for Macroscopic Spherical Solid Particles. *J. Colloid. Interface Sci.* **2000**, *223*, 133–138. [[CrossRef](#)]
57. Israelachvili, J.N. Van der Waals Forces between Particles and Surfaces. *Intermol. Surf. Forces* **2011**, *2011*, 253–289.

58. Winterton, R.H.S. Van der Waals forces. *Contemp. Phys.* **1970**, *11*, 559–574. [[CrossRef](#)]
59. Evstigneyev, E.I.; Yuzikhin, O.S.; Gurinov, A.A.; Ivanov, A.Y.; Artamonova, T.O.; Khodorkovskiy, M.A.; Bessonova, E.A.; Vasilyev, A.V. Study of Structure of Industrial Acid Hydrolysis Lignin, Oxidized in the H₂O₂-H₂SO₄ System. *J. Wood Chem. Technol.* **2016**, *36*, 259–269. [[CrossRef](#)]
60. Mayer-Laigle, C.; Rajaonarivony, R.K.; Rouau, X.; Fabre, C. Properties of biomass powders resulting from the fine comminution of lignocellulosic feedstocks by three types of ball-mill set-up. *Open Res. Eur.* **2022**, *1*, 125.
61. Bangar, S.P.; Singh, A.; Ashogbon, A.O.; Bobade, H. Ball-milling: A sustainable and green approach for starch modification. *Int. J. Biol. Macromol.* **2023**, *237*, 124069. [[CrossRef](#)]
62. Cavallini, C.M.; Franco, C.M.L. Effect of acid-ethanol treatment followed by ball milling on structural and physicochemical characteristics of cassava starch. *Starch/Staerke* **2010**, *62*, 236–245. [[CrossRef](#)]
63. Moraes, J.; Alves, F.S.; Franco, C.M.L. Effect of ball milling on structural and physicochemical characteristics of cassava and Peruvian carrot starches. *Starch/Staerke* **2013**, *65*, 200–209. [[CrossRef](#)]
64. Chambon, C.L.; Verdía, P.; Fennell, P.S.; Hallett, J.P. Process intensification of the IonoSolv pretreatment: Effects of biomass loading, particle size and scale-up from 10 mL to 1 L. *Sci. Rep.* **2021**, *11*, 1–15. [[CrossRef](#)]
65. Sathasivam, K.; Haris, M.R.H.M. Thermal properties of modified banana trunk fibers. *J. Therm. Anal. Calorim.* **2012**, *108*, 9–17. [[CrossRef](#)]
66. Fisher, T.; Hajaligol, M.; Waymack, B.; Kellogg, D. Pyrolysis behavior and kinetics of biomass derived materials. *J. Anal. Appl. Pyrolysis* **2002**, *62*, 331–349. [[CrossRef](#)]
67. Kabir, M.M.; Wang, H.; Lau, K.T.; Cardona, F. Chemical treatments on plant-based natural fibre reinforced polymer composites: An overview. *Compos. Part B Eng.* **2012**, *43*, 2883–2892. [[CrossRef](#)]
68. Elango, B.; Shirley, C.P.; Okram, G.S.; Ramesh, T.; Seralathan, K.K.; Mathanmohun, M. Structural diversity, functional versatility and applications in industrial, environmental and biomedical sciences of polysaccharides and its derivatives—A review. *Int. J. Biol. Macromol.* **2023**, *250*, 11. [[CrossRef](#)] [[PubMed](#)]
69. Monteiro, P.A.S.; Braz, C.E.M.; Seleguin, P.; Polikarpov, I.; Cruz, G.; Crnkovic, P.M. Thermal and Morphological Evaluation of Chemically Pretreated Sugarcane Bagasse. *World Acad. Sci. Eng. Technol.* **2013**, *78*, 1324–1329.
70. Berglund, L.; Noël, M.; Aitomäki, Y.; Öman, T.; Oksman, K. Production potential of cellulose nanofibers from industrial residues: Efficiency and nanofiber characteristics. *Ind. Crops Prod.* **2016**, *92*, 84–92. [[CrossRef](#)]
71. Kathirselvam, M.; Kumaravel, A.; Arthanarieswaran, V.P.; Saravanakumar, S.S. Isolation and characterization of cellulose fibers from *Thespesia populnea* barks: A study on physicochemical and structural properties. *Int. J. Biol. Macromol.* **2019**, *129*, 396–406. [[CrossRef](#)]
72. Thomas, M.G.; Abraham, E.; Jyotishkumar, P.; Maria, H.J.; Pothan, L.A.; Thomas, S. Nanocelluloses from jute fibers and their nanocomposites with natural rubber: Preparation and characterization. *Int. J. Biol. Macromol.* **2015**, *81*, 768–777. [[CrossRef](#)]
73. Phanthong, P.; Guan, G.; Ma, Y.; Hao, X.; Abudula, A. Effect of ball milling on the production of nanocellulose using mild acid hydrolysis method. *J. Taiwan. Inst. Chem. Eng.* **2016**, *60*, 617–622. [[CrossRef](#)]
74. Heritage, K.J.; Mann, J.; Roldan-Gonzalez, L. Crystallinity and the structure of celluloses. *J. Polym. Sci. Part A Gen. Pap.* **1963**, *1*, 671–685. [[CrossRef](#)]
75. Zhu, G.; Wang, Y.; Tan, X.; Xu, X.; Li, P.; Tian, D.; Jiang, Y.; Xie, J.; Xiao, H.; Huang, X.; et al. Synthesis of cellulose II-based spherical nanoparticle microcluster adsorbent for removal of toxic hexavalent chromium. *Int. J. Biol. Macromol.* **2022**, *221*, 224–237. [[CrossRef](#)]

Disclaimer/Publisher’s Note: The statements, opinions and data contained in all publications are solely those of the individual author(s) and contributor(s) and not of MDPI and/or the editor(s). MDPI and/or the editor(s) disclaim responsibility for any injury to people or property resulting from any ideas, methods, instructions or products referred to in the content.